Binding of a Distamycin–Ellipticine Hybrid Molecule to DNA and Chromatin: Spectroscopic, Biochemical, and Molecular Modeling Investigations†

Catherine Bourdouxhe,‡ Pierre Colson,‡ Claude Houssier,‡ Jian-Sheng Sun,§ Thérèse Montenay-Garestier,§ Claude Hélène,§ Christian Rivalle,‖ Emile Bisagni,‖ Michael J. Waring,⊥ Jean-Pierre Hénichart,# and Christian Bailly*,#

Laboratoire de Chimie Macromoléculaire et Chimie Physique, Université de Liège, Sart-Tilman (B6), Liège 4000, Belgium, Laboratoire de Biophysique, Muséum National d'Histoire Naturelle, CNRS UA 481–INSERM U201, 43 rue Cuvier, 75005 Paris, France, CNRS URA 1387, Laboratoire de Synthèse Organique, Institut Curie-Biologie, Bât. 110-112, 15 rue G. Clemenceau, 91405 Orsay, France, Department of Pharmacology, University of Cambridge, Tennis Court Road, Cambridge CB2 1QJ, U.K., and INSERM U16, Place de Verdun, 59045 Lille Cedex, France

Received June 23, 1992; Revised Manuscript Received September 9, 1992

ABSTRACT: A bifunctional molecule in which an ellipticine chromophore is attached to a distamycin residue via a diaminopropyl tether has been designed and synthesized in the expectation of creating a hybrid molecule capable of bidentate binding to DNA by both intercalation and minor-groove interactions. The strength and mode of binding to DNA of this conjugate have been studied by means of circular and linear dichroism as well as by stopped-flow kinetics and measurements of reactivity toward a chemical probe. The results converge to reveal that the ellipticine moiety of the hybrid largely dominates the binding reaction with DNA. In the presence of chromatin, the hybrid molecule binds preferentially to the internucleosomal DNA, a preference dictated by its intercalating chromophore. Theoretical computations were performed on the comparative complexation energies of distamycin, the ellipticine derivative, and the hybrid ligand with a B-representative octanucleotide, $d(GCATATGC)_2$. The best binding configuration of the ellipticine derivative locates its aminoalkyl side chain in the minor groove where distamycin is also present. The molecular modeling analysis fully supports the involvement of a bimodal binding process for the hybrid and reveals that the binding of the conjugate to DNA favors a pronounced bending toward the minor groove. This effect is attributed to intercalation of the ellipticine chromophore. An interesting link is established between the DEPC reactivity experiments and the theoretical computations, suggesting that DEPC can be used as a probe for drug-induced DNA bending. On the basis of these results, we propose the design of a new hybrid ligand bearing an additional positively-charged amidine side chain to confer higher DNA-binding affinity.

Interaction with DNA, inhibition of replicative enzymes or DNA repair systems, poisoning effects directed toward topoisomerases, and many other processes such as free radical production or binding to membranes are interrelated phenomena which very likely contribute to the pharmacological properties of numerous antiviral and antitumor agents. These different potential molecular targets cannot all be considered together as a basis to synthesize new drugs. However, the rational design of potential new antitumor drugs is an important and difficult exercise which demands imaginative chemistry applied to a well-defined target. Our choice, for good reason, is DNA.

Distamycin is a well-characterized pseudopeptide isolated from a strain of *Streptomyces distacillus* that exhibits a wide spectrum of antimicrobial, antiviral, and antitumor properties. It is formed from the repetition of three *N*-methylpyrrolecarboxamide residues (Figure 1b) that produce an arc conformation in the planar molecule. This arc matches to some extent the turn of the DNA double helix. The drug binds strongly to AT-rich regions within the minor groove of DNA without gross helical distortion and acts to block the template function of DNA (Zimmer & Wähnert, 1986). Ellipticine is an antitumor alkaloid isolated from plants growing in the Pacific islands (Hartwell & Abbott, 1969). Molecules of the ellipticine family consist of planar chromophores derived from 6*H*-pyridocarbazole which intercalate into DNA (Le Pecq et al., 1974; Kohn et al., 1975) and which can also induce DNA strand breakage (Paoletti et al., 1979; Zwelling et al., 1982). The 1-aminopropylamino ellipticine derivative used in this study (Figure 1a) is several times more cytotoxic than the natural ellipticine against a number of murine tumor cells (Ducrocq et al., 1980; Larue et al., 1988). This functionalized derivative intercalates preferentially at GC-rich sites (Bailly et al., 1990a), a property attributable to its 9-methoxy substituent (Schwaller et al., 1989). The protonated alkylamino side chain attached to the aromatic ring system enhances the affinity for DNA and also provides opportunities for introducing functional groups onto the ellipticine chromophore. Indeed, linkage to an oligonucleotide via the free amino group has produced an efficient triple-

† This work was done under the support of Research Grant FRFC convention 2.4503.90 and 2.4501.91 from the Fonds National de la Recherche Scientifique (to P.C. and C. Houssier); (to J.-S.S., T.M.-G., and C. Hélène) from the Centre National de la Recherche Scientifique (CNRS) and the Institut National de la Santé et de la Recherche Médicale (INSERM); (to C.R. and E.B.) from the CNRS and the Institut Curie; (to M.J.W.) from the Cancer Research Campaign, the Medical Research Council, and the Royal Society; (to J.-P.H. and C. Bailly) from the INSERM and the Association pour la Recherche sur le Cancer. Support by the "convention INSERM-CFB" is acknowledged. C. Bourdouxhe is the recipient of an IRSIA fellowship.

* Address correspondence to this author.
‡ Université de Liège.
§ Muséum d'Histoire Naturelle.
‖ Institut Curie.
⊥ University of Cambridge.
INSERM.

0006-2960/92/0431-12385$03.00/0

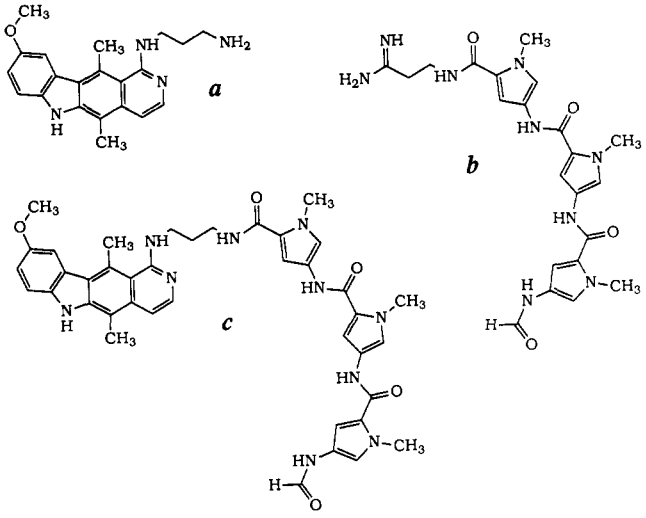

FIGURE 1: Chemical structure of the ellipticine derivative (a), distamycin (b), and the distamycin–ellipticine hybrid, Distel (c).

helix-forming artificial photoendonuclease (Perrouault et al. 1990; Le Doan et al., 1991).

This ellipticine derivative has now been linked to a distamycin-like entity bearing a free carboxyl end in order to form a hybrid molecule, henceforth called Distel (Figure 1c), designed to bind to DNA by both intercalation and minor-groove interactions. The resulting hybrid molecule is thus constructed from two well-known DNA-binding domains differing in their mode of binding to DNA, their sequence selectivity, and their biological properties. Such a molecule typifies the concept of ligands having mixed binding functions (Bailly & Hénichart, 1991), which we hope will prove useful as an independent approach to the development of potential gene probes or therapeutic drugs. To gain a proper understanding of the molecular mechanism of action of this hybrid molecule, a detailed knowledge of its mode of binding to DNA is mandatory. This should then serve as a starting point for computer-aided drug design studies, which may eventually lead to the development of analogs with better DNA-binding properties and hopefully with a higher therapeutic effect.

A first report on the strength and mode of binding to DNA of Distel together with data on its sequence selectivity was recently presented (Bailly et al., 1992b). Spectrophotometric measurements led to the conclusion that, as expected from the chemical structure, intercalation of the ellipticine moiety and groove binding of the distamycin moiety are both implicated in the binding of the hybrid to DNA. However, DNase I footprinting investigations aimed at detecting the sequence selectivity of binding revealed a closely similar distribution of binding sites for the hybrid and for the ellipticine moiety alone. Footprints of the distamycin moiety were practically not distinguishable. Thus, an interesting discrepancy is evident between the spectrophotometric measurements and the footprinting data and we are confronted with a more complicated situation than originally anticipated. That is the problem which we address here.

The present investigation began with an attempt to delineate further the role of the distamycin moiety as opposed to the chromophoric ellipticine moiety in an attempt to gain insight into the molecular pharmacology of each functionality. Circular and electric linear dichroism experiments were performed with the hybrid, reinforced by competition experiments with distamycin and the functionalized ellipticine derivative. Kinetic data, obtained by monitoring the SDS-driven dissociation of drug–DNA complexes by stopped-flow measurements, were also determined, along with an assessment of drug effects on the DNA conformation by studies of reactivity toward chemical probes. All these experiments provided the input for molecular mechanics calculations from which the structure of the hybrid–DNA complex was derived. Thus, a complete description is given of the structural features of the DNA–Distel complex with all its pecularities.

Additionally, in order to model more pertinently the binding process that takes place in vivo, we have sought information about the binding of the hybrid molecule and its constituents to DNA packed into a nucleosomal chromatin structure. Mechanisms that alter the conformation of DNA and chromatin in living cells are likely to affect the efficiencies of transcription, replication, recombination, and DNA repair. It is thus important to know how the drug behaves in the presence of chromatin compared to DNA. Finally, the relevance of our experimental and theoretical findings for the design of other hybrid molecules is discussed.

MATERIALS AND METHODS

Chemicals. Distamycin A hydrochloride was purchased from Boehringer (Mannheim, Germany); stock solutions were prepared in water. The ellipticine derivative 1-(3-aminopropyl)amino-5,11-dimethyl-9-methoxy-6*H*-pyrido[4,3-*b*]carbazole was synthesized as described (Ducrocq et al., 1980). A stock solution (1 mM) of this compound was prepared in methanol since it is practically insoluble in water. This solution was stored at −20 °C in the dark and diluted to working concentrations prior to use. The synthesis of the hybrid drug Distel, together with complete spectral characterization, will be reported in a chemical communication. Briefly, the drug was obtained from the coupling of 4-[[[4-[[[4-(formylamino)-1-methylpyrrol-2-yl]carbonyl]amino]-1-methylpyrrol-2-yl]-carbonyl]amino]-1-methylpyrrole-2-carboxylic acid (Bailly et al., 1989) with the ellipticine derivative cited above (Ducrocq et al., 1980). Stock solutions of this compound were prepared in dimethylformamide before subsequent dilutions with water. The final dimethylformamide concentration in experiments did not exceed 1–2% (v/v). Drug concentrations were determined spectrophotometrically, applying molar absorption coefficients given in Table I. Electrophoretic reagents [Tris, acrylamide, bis(acrylamide), urea, *N,N,N′,N′*-tetramethylethylenediamine (TEMED), and ammonium persulfate] were from BDH. X-ray films and developing chemicals were from Kodak. All other chemicals were analytical-grade reagents.

Biochemicals. Calf thymus (CT) DNA (highly polymerized, sodium salt) was purchased from Sigma Chemical Co., deproteinized twice with sodium dodecyl sulfate (SDS), and precipitated with ethanol. The stock solution was extensively dialyzed against the appropriate buffer. The plasmid pBS (Stratagene, La Jolla, CA.) was digested to completion with *Pvu*II followed by *Ava*I restriction enzymes (Boehringer, Mannheim) giving a 253 base pair *Pvu*II–*Ava*I DNA fragment suitable for 3′-end labeling. Two ethanol precipitations were effected before the 3′-end labeling with [α-^{32}P]dCTP (6000 Ci/mmol, New England Nuclear) and reverse transcriptase (Pharmacia) under standard conditions (Bailly et al., 1990a, 1992b,c). After electrophoresis on polyacrylamide gels, the 253-bp band was identified by autoradiography, excised, and isolated by elution in 500 mM ammonium acetate and 10 mM magnesium acetate buffer. The preparation of chicken erythrocyte (CE) chromatin fragments followed the procedures described earlier (Hagmar et al., 1989). In the ionic strength conditions used for electric linear dichroism measurements (1 mM cacodylate, pH 6.5), chromatin (10–80 nucleosomes long)

Table I: Spectroscopic Data, Binding Constants, and Estimates of Site Size for Distamycin, the Ellipticine Derivative, and Distel Bound to Calf Thymus DNA and Chicken Erythrocyte Chromatin[a]

	ϵ^b	λ_{max} (nm)			λ isosbestic point		DNA[d]				chromatin[d]			
	(M^{-1} cm^{-1})	free	DNA	chrom	DNA	chrom	n_1	K_1 (M^{-1})	n_2	K_2 (M^{-1})	n_1	K_1 (M^{-1})	n_2	K_2 (M^{-1})
ellipticine derivative	48 000	306	318	317	305[e] 317[f]	314[f]	0.048	1.5×10^8	0.32	3.0×10^5	0.16	1.3×10^7	0.54	6.2×10^4
distamycin	35 000	302	320	320			0.14	3.5×10^6	0.75	4.3×10^4	0.13	4.0×10^6	0.35	3.5×10^4
Distel	81 000	306	322	315	307[e] 318[f]		0.035	9.0×10^7	0.38	9.4×10^4	0.19	5.0×10^6		

[a] Association constants and parameters of site size were estimated using a two-site model which assumes the existence of two independent noncooperative types of binding and which was found to fit satisfactorily the binding curves for the three compounds studied. [b] ϵ = molar extinction coefficient. [c] λ^{max} = absorption maximum. [d] K = association constant, n = number of ligand binding sites per nucleotide. [e] At D/P (drug/DNA phosphate ratio) < 0.3. [f] At D/P > 0.3.

is mostly present as the 10-nm fiber. DNA concentrations were determined at 260 nm using molar extinction coefficients of 6600 and 6800 M^{-1} cm^{-1} for isolated DNA and chromatin, respectively.

Absorption Spectroscopy, Binding Constants, and Estimates of Site Size. Absorption spectra were recorded on a Perkin-Elmer Lambda 5 spectrophotometer using a 10-mm optical path length. Titrations of the drugs with DNA, covering a large range of drug/DNA phosphate ratios (D/P), were performed by adding aliquots of a concentrated DNA or chromatin solution to a drug solution at constant ligand concentration (10 μM). Binding constants were determined using experimental spectrophotometric readings from absorbance titration experiments conducted at 325 nm with distamycin, 322 nm with the ellipticine derivative, and 323.5 nm with the hybrid molecule. For each ligand the apparent association constant(s) K (M^{-1}) and numbers of sites per nucleotide n were estimated from Scatchard plots using two models: the noncooperative ligand binding model of McGhee and von Hippel (1974) and a two-site model which assumes the existence of two independent noncooperative types of binding sites (Bailly et al., 1990b). Although the McGhee–von Hippel model might appear more appropriate for a ligand which certainly covers several sites, no satisfactory adjustment of the parameters to fit the experimental data could be obtained. By contrast, the two-site model was found to provide a very good fit to the experimental data for both Distel–DNA and ellipticine derivative–DNA complexes. With distamycin, good curve fitting was obtained with both the McGhee–von Hippel model and the two-site model in the presence of DNA, while only the two-site model provided acceptable fitting in the presence of chromatin. The program Enzfitter (Elsevier Biosoft) (Leatherbarrow, 1990) was used to obtain the best fit of the data to each of these two models.

Circular dichroism (CD) measurements were recorded on a Jobin-Yvon Mark V dichrograph interfaced to a Silex microcomputer. Solutions of drugs and/or nucleic acids were scanned in 1-cm quartz cuvettes. Measurements were made by progressive addition of DNA (or chromatin) to a pure ligand solution to get the desired drug/DNA ratios. Results are expressed in molar circular dichroism $\Delta\epsilon = \Delta A/lc$, where ΔA is the circular dichroism amplitude, l is the cell path length, and c is the ligand concentration.

Electric linear dichroism (ELD) measurements were carried out in 1 mM sodium cacodylate, pH 6.5, in a 10-mm path length Kerr cell with 1.5-mm electrode separation, using the instrumentation previously described (Fredericq & Houssier, 1973; Houssier, 1981; Bailly et al., 1990b). The conductivity of all the solutions was measured directly in the electrooptical cell with a Metrohm conductimeter Model E527 and never exceeded 2 mS. This electrooptical method exploits the fact that, under the influence of a short electric field pulse, the DNA molecule becomes oriented, rendering the solution optically anisotropic (Fredericq & Houssier, 1973; Houssier, 1981).

Kinetic measurements were conducted with a Bio-Logic SFM-3 stopped-flow spectrometer coupled to Bio-Kine V3.0 software for data acquisition and analysis. Single-wavelength kinetic records of voltage versus time were collected and converted to absorbance. Typically, 8–10 runs were collected and averaged by the computer to improve the signal-to-noise ratio. Dissociation reactions were monitored by mixing equal volumes (100 μL) of a DNA–drug complex with a 1% SDS solution according to the method of Müller and Crothers (1968). In the presence of SDS, added to sequester the unbound ligand and to drive the dissociation reaction, the drug spectra underwent a red shift as well as an increase in extinction coefficient attributed to a partial self-association of the drug in solution. The wavelength used to carry out the measurements (314 nm) was chosen around the maximum drug absorption in SDS solution. Checks were carried out to make sure that no time-resolvable changes occurred on mixing free drug solutions with SDS. The dead time of the instrument was 3 ms. Digitized traces were fitted to multiple exponentials by a least-squares fitting procedure.

Competition experiments were undertaken to determine whether distamycin and the ellipticine derivative would mutually interfere in their binding to DNA when they were not integrated in the hybrid molecule. Both circular and electric linear dichroism techniques were used. Measurements were made at two D/P ratios for one ligand (held constant) while the other ligand was progressively added to the complex. The two D/P ratios were not randomly chosen: at a D/P ratio of 0.1, the ellipticine derivative is mainly intercalated between DNA base pairs, while at a D/P ratio of 0.5, a partial external binding process is also present. CD spectra were recorded between 220 and 370 nm and were corrected for dilution effects. ELD measurements were carried out at 320 and 330 nm.

Diethyl Pyrocarbonate Footprinting, Electrophoresis, and Autoradiography. The reaction with diethyl pyrocarbonate (DEPC) was performed essentially according to a published protocol (Portugal et al., 1988). One microliter of ^{32}P-labeled DNA was incubated with 19 μL of the drug solution (maximal final methanol concentration 5%) for 15 min at 37 °C. The mixture was kept at 0 °C for 3 min before addition of 1 μL of DEPC (Sigma). Samples were incubated at room temperature for a further 15 min with agitation. The reaction was terminated by addition of sodium acetate to 0.3 M followed by ethanol precipitation and a 70% ethanol wash. The pellet was resuspended in 30 μL of 1 M piperidine, heated at 90 °C for 15 min, lyophilized, and resuspended in 4 μL of 80% formamide containing 10 mM EDTA, 0.1% bromophenol blue, and 0.1% xylene cyanol. The cleavage products of the DEPC/

piperidine reactions were analyzed on 0.3-mm-thick, 8% polyacrylamide gels containing 8 M urea and Tris–borate–EDTA buffer (8.9 mM Tris base, 8.9 mM boric acid, and 2.5 mM Na_2EDTA, pH 8.3). After 2 h of electrophoresis at 1400 V, the gels were fixed in 10% acetic acid, transferred to Whatman 3MM paper, dried under vacuum at 80 °C, and subjected to autoradiography (Kodak, X-OMat AR) at −70 °C with an intensifying screen. Methylation by dimethylsulfate and reaction with potassium tetrachloropalladinate were carried out basically as described by McLean and Waring (1988). Quantitative analysis of the gel electrophoresis profiles was performed by integration of the area under each peak, using a computer program specially developed for this purpose (Smith & Thomas, 1990).

Molecular Modeling. Conformational energy minimization was performed with the JUMNA (junction minimization of nucleic acids) program package (Lavery, 1988), which used helicoidal coordinates particularly suitable for nucleic acids. Recent developments of the JUMNA program package (JUMNA IV) allowed us to include any number of nonbonded ligands into the calculations with the help of the NChem (nucleotide chemistry) program. The ellipticine derivative, distamycin, and Distel conjugate molecules were built using the Insight II graphic program developed commercially by Biosym and then charged and analyzed by NChem to prepare a data file containing geometrical parameters, atomic charges, and flexibility information for use in the JUMNA program. Charges of ligands were calculated with a Huckel–Del Re procedure which was parameterized on the basis of quantum mechanical calculations (Lavery et al., 1984). Neither water nor counterions were explicitly included in this calculation. Their effects were simulated by using a sigmoidal distance-dependent dielectric function (Lavery et al., 1986), and by assigning half a charge to the phosphate group.

The first step in the computing procedure required building up the DNA fragment, which consisted of eight base pairs in double-helical arrangement [$d(GCATATGC)_2$], positioning the various nucleotides by means of their helicoidal coordinates relative to the global axis system. Helicoidal coordinates were derived from published data obtained by crystallography on the B-DNA double helix (Arnott et al., 1980). In order to create an intercalation site, the rise parameter was doubled at the expected site, and the twist subsequently reduced. The interactive docking of the ligand–DNA complex was achieved manually by using Insight II software to avoid close contacts. In early stages of minimization, the helicoidal variables and/or the sugar–phosphate backbone, as well as ligand variables, could be locked. Minimization was performed by successively decreasing the number of constraints. Finally all variables were freed to evolve until the energy convergence criterion was reached. We have checked that the results were not affected by the order under which the constraints were released. To ensure that the energy-minimized models were suitable, several starting structures were used. These computations were performed on a Silicon Graphics 4D/120GTXB workstation and the molecules were visualized with the help of Insight II fully interfaced with JUMNA. The structures obtained after minimization were analyzed by the CURVE (Lavery & Sklenar, 1989) program, which determined the helicoidal parameters of all the bases with respect to a global axis derived by the least-squares fit.

RESULTS AND DISCUSSION

Absorption Spectroscopy. Binding constants, estimates of site size, and other spectroscopic data for drug binding to DNA and chromatin are given in Table I. As recently reported (Bailly et al., 1992b), DNA–ellipticine derivative spectra exhibit an isosbestic point around 305 nm for low drug to DNA (D/P) ratios, which corresponds to total intercalation observed in the presence of a large excess of DNA. The isosbestic point at 305 nm disappears at high D/P ratios and another isosbestic point is observed at 317 nm, reflecting progressive external binding to DNA. When titrated with chromatin, the ellipticine derivative displays no isosbestic point at low D/P ratios, indicating that changes have occurred in the chromophore intercalation conditions with respect to those observed with DNA. Distamycin does not show any isosbestic point upon binding to DNA or chromatin. This may reflect a heterogeneous interaction consistent with minor-groove binding (Zimmer & Wähnert, 1986). Indeed, the groove-binding process occurs in a sequence-dependent manner at numerous sites along the double helix. The heterogeneity of the DNA leads to a heterogeneous binding environment. In the presence of DNA, the hybrid molecule Distel behaves like the ellipticine derivative at low D/P ratios (an isosbestic point is observed at 307 nm, indicative of intercalation) and like distamycin at higher D/P ratios (disappearance of the isosbestic point, indicative of external binding). In the presence of chromatin no clear isosbestic point is observed.

The binding data in Table I indicate that for both the ellipticine derivative and the hybrid compound the product $K_1 n_1$ corresponding to the high-affinity sites is decreased by a factor of about 3 in the case of chromatin compared to DNA. This reflects the decreased DNA accessibility in chromatin structure compared to protein-free DNA. Distamycin displays no significant change, suggesting that its access to the minor groove is more or less the same in DNA and chromatin. This corroborates previous studies showing that 80–90% of the DNA is still accessible to distamycin in chromatin fibers (Zimmer & Wähnert, 1986). The same observation holds true for Distel; its accessibility to DNA is apparently not disturbed by the presence of histones.

The equilibrium constants measured for the binding of the three ligands to chromatin differ from those determined with DNA. The most significant differences are observed with the ellipticine derivative; the two binding constants for chromatin are much lower, probably indicative of less effective intercalation. On the other hand, in the presence of DNA or chromatin the binding constants for distamycin are very similar. Thus again, the minor-groove binder appears insensitive to the presence of proteins bound to DNA. The hybrid Distel exhibits an intermediate behavior with respect to its two components. Its binding constants to chromatin are both reduced compared to DNA, most particularly the constant K_1, showing that the high affinity of Distel for its best sites is reduced in the presence of chromatin.

Circular Dichroism (CD). The ligands under investigation do not exhibit intrinsic optical activity but become optically active when they bind to a macromolecular template such as DNA or chromatin. As displayed in Figure 2, the CD signals measured with the ellipticine derivative and distamycin in the presence of increasing DNA concentrations (i.e., decreasing D/P ratios) are quite different. The CD signal of the ellipticine derivative monitored at 320 nm first increases with decreasing D/P ratios until a D/P value of 0.4–0.5 is reached, and then it rapidly decreases to become negligible at a D/P value lower than 0.2. The disappearance of the CD peak at this D/P ratio is attributable to decrease of excitonic coupling arising from a distance increase between adjacent molecules. Such biphasic evolution of the CD signal of the ellipticine derivative with

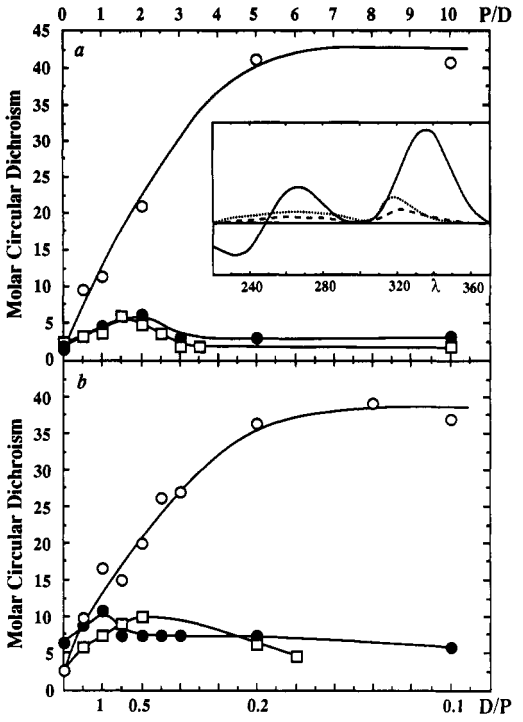

FIGURE 2: Variations in molar circular dichroism $\Delta\epsilon$ (ΔA over drug concentration for 1-cm cell path length) with decreasing drug/DNA ratios for distamycin (○), the ellipticine derivative (□), and Distel (●) bound (a) to calf thymus DNA and (b) to chicken erythrocyte chromatin. λ = 330 nm for distamycin; λ = 320 nm for the ellipticine and Distel. The inset shows typical CD spectra of complexes of distamycin (solid line), ellipticine derivative (dotted line), and Distel (dashed line) with calf thymus DNA at a drug/DNA ratio of 0.5.

decreasing D/P ratios is characteristic of an excitonic coupling and fully consistent with an intercalative mode of binding to DNA. Similar variation of molar dichroism with the D/P ratio has been reported with other intercalating agents such as ethidium bromide (Houssier et al., 1974) and acridine orange (Fredericq & Houssier, 1972). By contrast, the distamycin-induced CD signal, due to asymmetry of the binding site, is much larger. The signal increases rapidly when DNA is added to the drug solution (i.e., with decreasing D/P) until total binding of distamycin to DNA is reached. If referred to bound ligand concentration, the molar circular dichroism ($\Delta\epsilon$ expressed in M^{-1} cm^{-1}) remains roughly constant over the whole range of D/P covered, which supports the molecular origin of the effect. Effectively, at D/P = 1 the molar circular dichroism, corrected by taking into account the percentage of free distamycin (65–70%), rises to a value of 35–40 M^{-1} cm^{-1}, in agreement with the value measured in the region of total binding (at low D/P values) where the signal tends to level off. A similar D/P dependence of the dichroism induced in distamycin by the presence of DNA was reported previously (Zimmer, 1975; Luck et al., 1977). Thus, in the presence of DNA, distamycin and the ellipticine derivative exhibit clear and distinctive CD signals in their respective absorption bands. The CD technique should therefore be suitable for estimating the contribution of each part of the hybrid in the binding reaction with DNA even if, as shown in Figure 2 (inset), the broad signal of distamycin overlaps that of the ellipticine derivative. The overlap of these two absorption bands represents an unavoidable problem encountered throughout the entire spectroscopic analysis, which does tend to complicate the interpretation of the results.

The CD signals observed with Distel–DNA complexes closely resemble those obtained with ellipticine derivative–DNA complexes (Figure 2, inset). The curves of molar dichroism vs D/P ratio are very similar for the ellipticine derivative and Distel (Figure 2). The large CD signal characteristic of distamycin, centered at 330 nm, is apparently completely quenched with the hybrid. These CD results suggest that the ellipticine moiety of the hybrid behaves more or less like the ellipticine derivative alone. In other words, the distamycin moiety of the hybrid does not noticeably hinder the intercalative binding of the ellipticine part. On the contrary, minor-groove binding of the tris(pyrrole) portion of the hybrid is clearly affected by the combination with the planar heterocyclic ellipticine chromophore, which appears to dominate the DNA-binding reaction. However, the absence of a distamycin-like intense CD signal at 330 nm with the hybrid does not necessarily mean that binding within the minor groove has disappeared. The results of the CD experiments simply reveal that the binding of the pseudopeptidic moiety of the hybrid occurs in a different way compared to distamycin alone.

The optical activity induced when the three drugs interact with chromatin is similar to that observed with DNA (Figure 2b). It can thus be assumed that histone proteins do not disturb locally the binding modes of these three drugs. Although the CD spectra do not identify the type of DNA complex formation, they clearly illustrate that ellipticine derivative–DNA and Distel–DNA complexes fall into a similar conformational class that is different from that of the distamycin–DNA complex.

Electric Linear Dichroism (ELD). In these experiments the biological polymer (DNA or chromatin) is oriented by an applied electric field and the dichroism in the region of the absorption bands of the ligand bound to DNA is probed using linearly polarized light. The intensity of the ELD signal measured in the absorption band of the ligand is dependent on the orientation of the drug relative to the direction of the macromolecular axis.

The results obtained with DNA are reported in Figure 3a. The ellipticine derivative exhibits a negative reduced dichroism ($\Delta A/A$ = –0.55 at 310 nm), in agreement with an orientation of the ellipticine chromophore parallel to the DNA base pairs, a configuration consistent with an intercalative binding mode. As for distamycin, the ELD signal is positive and its amplitude ($\Delta A/A$ = +0.5 at 330 nm) fits a minor-groove binding process. The ELD spectrum of the hybrid–DNA complex is intermediate between that of its parent compounds and may be supposed to reflect the contribution of the two moieties of the hybrid. The hybrid–DNA spectrum displays a negative region in the 290–330-nm band, indicating intercalation of the ellipticine chromophore between DNA base pairs together with a weakly positive region in the 330–350-nm band, presumed to reflect groove binding of the tris(pyrrole) part of the hybrid. Note that the Distel–DNA ELD spectrum differs from the "theoretical" difference spectrum obtained by adding the distamycin ELD spectrum to that of the ellipticine derivative.

The organization of chromatin in nucleosomes leads to lower global orientation of DNA base pairs with respect to the chromatin fiber axis. Accordingly, the reduced dichroism value of chromatin ($\Delta A/A$ = –0.05 at 260 nm and 12.5 kV/cm) is about 10-fold lower than that of protein-free DNA under the same conditions ($\Delta A/A$ = –0.5). In the presence of chromatin, the ellipticine derivative shows negative dichroism at 310 nm which is 5 times higher than the dichroism measured at 260 nm (Figure 3b), where the measured dichroism is close to that expected for free chromatin. It is worth noting that the contribution of the ligand to the total

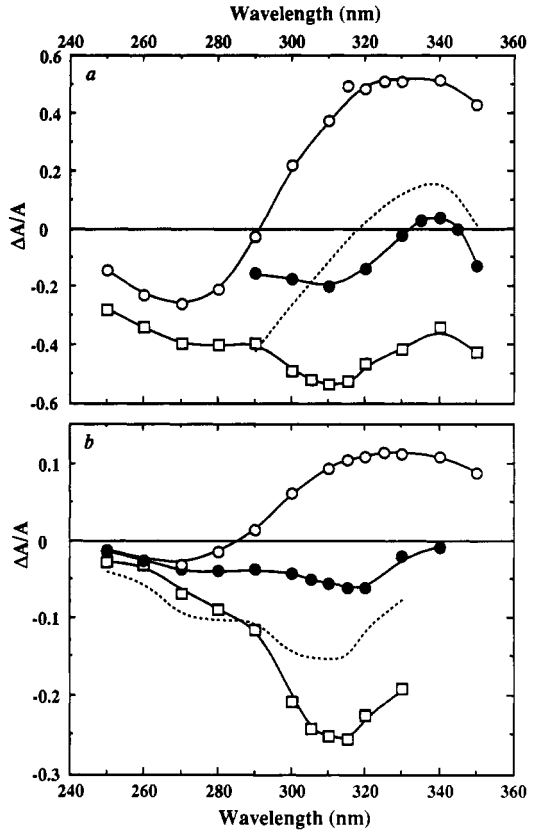

FIGURE 3: Reduced electric dichroism ($\Delta A/A$) spectra of distamycin (○), the ellipticine derivative (□), and Distel (●) bound (a) to calf thymus DNA and (b) to chicken erythrocyte chromatin, at 12.5 kV/cm and at a drug/DNA ratio corresponding to total binding (indicated in Table I). Dashed spectra correspond to the sum of the reduced dichroism values measured for the distamycin– and ellipticine–DNA complexes.

absorption at 260 nm is less than 10%, so that the dichroism measured at this wavelength is mainly due to DNA or chromatin bases and can therefore be compared to the dichroism of the macromolecule alone. The intense negative dichroism at 310 nm could be attributed either to nucleosome unwinding that occurs upon drug intercalation (McMurray & van Holde, 1986, 1991) or to prominent binding of the ellipticine derivative to the DNA linker region, the base orientation of which is higher than that of nucleosomal DNA in extended chromatin fibers and in zigzag chains. The former possibility is unlikely since nucleosome unwinding would cause the amplitude of the dichroism around 260 nm to become more negative and to reach the same order of magnitude as in the ellipticine derivative band. The latter explanation is altogether more likely since the accessibility of the DNA linker region is much higher than that of DNA integrated in the nucleosome structure. Preferential binding to linker DNA should result in more negative dichroism values in the ligand absorption band, as observed. A similar propensity to intercalate preferentially into linker DNA has been reported with unsubstituted natural ellipticine (Larue et al., 1987) as well as with other simple intercalating agents such as ethidium (McMurray & van Holde, 1986, 1991) and methylene blue (Kubista et al., 1985; Hagmar et al., 1992).

In order to assess the localization of the ligands in chromatin (at a D/P of 0.1), we compared, at a given field strength, the ration R of the reduced dichroism of DNA over that of chromatin in the absorption bands of the bases (260 nm, where the macromolecule is mainly contributing to the dichroism) and of the three ligands (in the 310–330-nm range). The reduced electric dichroism, at any field strength, is given by the general relationship

$$(\Delta A/A) = (\Delta A/A)_s \Phi \quad (1)$$

where Φ is the orientation function ($0 \leq \Phi \leq 1$), which reflects the degree of orientation of the particles at a given field strength E and depends on the electric factors responsible for this orientation. The reduced dichroism at saturation, $(\Delta A/A)_s$ is related to the mean angle α of the transition moment of the chromophore with respect to the orientation axis of the particle. For DNA in double-helical structure, $(\Delta A/A)_s$ is given by

$$(\Delta A/A)_{s,h} = {}^3/_2(3\cos^2\alpha - 1) \quad (2a)$$

Since in chromatin the chromophoric groups are arranged in a superhelical structure, $(\Delta A/A)_s$ also depends on the superhelix pitch angle θ of the superhelix axis, and irrespective of the number of superhelical turns, one obtains [for details see Houssier (1981)]

$$(\Delta A/A)_{s,sh} = {}^3/_2(3\cos^2\alpha - 1)[(3\cos^2\theta - 1)/2] \quad (2b)$$

In eqs 2a and 2b, the subscripts sh and h refer to the superhelical and helical structures, respectively. At 260 nm, the ratio R is given by

$$R_{260} = \frac{(\Delta A/A)^{260}_{DNA}}{(\Delta A/A)^{260}_{CHR}} = \frac{\Phi_{DNA}}{\Phi_{CHR} C_\theta} \quad (3)$$

where Φ_{DNA} and Φ_{CHR} are the orientation functions for DNA and chromatin, respectively, while C_θ is the optical anisotropy factor, which takes into account the superhelical structure of chromatin (see eq 2b). This R_{260} ratio may be compared with a ratio similarly defined in the absorption bands of the ligands. For any drug, we can write in its absorption region

$$R_{drug} = \frac{(\Delta A/A)^{drug}_{DNA}}{(\Delta A/A)^{drug}_{CHR}} = \frac{\Phi_{DNA}}{\Phi_{CHR} C_\theta} \quad (4)$$

If the ligand is evenly distributed along the macromolecular chain, the two ratios defined in eqs 3 and 4 should have the same value at a given field strength. The larger the difference between these two ratios, the more selective is the localization of the ligand in chromatin.

As mentioned above, R_{260} is equal to 10 in the absence of drug. A similar value of R_{drug} would reflect a homogeneous distribution of the drug between both nucleosomal core particles and linker DNA (the same as for the base pairs). The R value for ellipticine is equal to 2, illustrating a clear preference for binding to the linker DNA given that the DNA linker constitutes about 20% of the total nucleosomal DNA of chicken erythrocytes.

The ELD spectrum of the distamycin–chromatin complex shows a maximum at 325 nm with a $\Delta A/A$ value of +0.1, so that $R_{distamycin}$ is equal to 5 (see Figure 3b). The latter value reflects a nonhomogeneous distribution of distamycin along the chromatin chain with a less marked preference for linker DNA than the ellipticine derivative. In other words, distamycin is partially located in the minor groove of nucleosomal core particles too. The hybrid compound Distel exhibits, in the presence of chromatin, an ELD spectrum intermediate between those of its two constituents, distamycin and the ellipticine derivative, but the observed spectrum differs significantly from that expected if a simple additive effect of distamycin and the ellipticine derivative were to take place (see Figure 3b). Nevertheless, the R_{Distel} value is equal to 4, which does seem to combine effects from each of its two

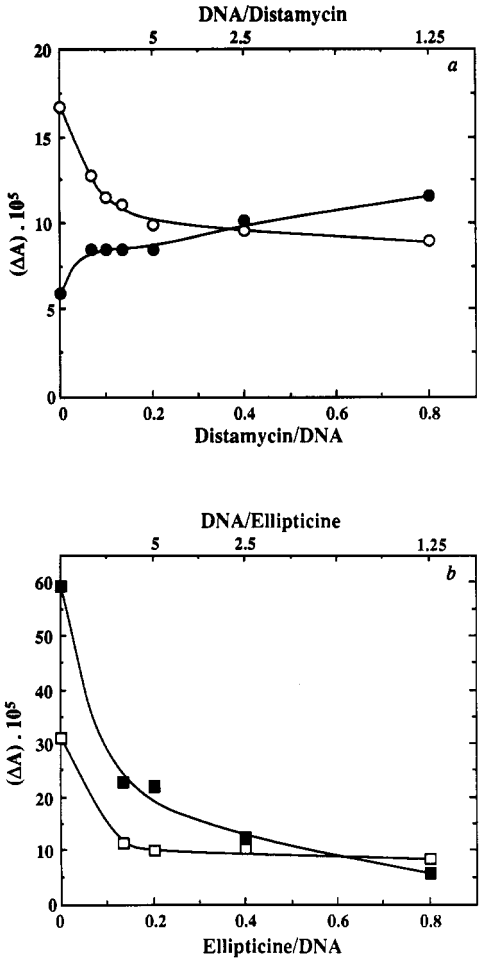

FIGURE 4: Changes in circular dichroism amplitudes (ΔA) at 320 nm (open symbols) and 330 nm (filled symbols) as a function of (a) distamycin addition to a solution of ellipticine–DNA complex at a fixed ratio of 0.5 and (b) ellipticine addition to a solution of distamycin–DNA complex at a fixed ratio of 0.5.

constituents. Thus, the comparison of the R values for the three ligands enables us to conclude a preference for binding to linker DNA in the following order: ellipticine derivative > Distel > distamycin.

Competition Experiments: (*A*) *Circular Dichroism.* Figure 4a shows the CD changes that occur when distamycin is progressively added to an ellipticine derivative–DNA complex at a fixed D/P ratio of 0.5. Conversely, Figure 4b shows the variation of the CD amplitude upon addition of the ellipticine derivative to a distamycin–DNA complex at the same constant D/P ratio. CD changes were recorded at two different wavelengths, 320 and 330 nm, in order to try to distinguish the role of the distamycin compared to that of the ellipticine moiety. At the lower wavelength, the CD signal results from the additive contributions of both the ellipticine derivative and distamycin, while at the higher wavelength the CD signal is mainly due to distamycin (see Figure 2a, inset). The CD signal at 330 nm increases slightly when distamycin is added to the ellipticine derivative–DNA complex (Figure 4a), but this increase is negligible compared to that obtained in similar experiments using an ellipticine derivative/DNA ratio of 0.1 (data not shown). This result reflects the fact that external binding of ellipticine, present at a D/P ratio of 0.5 (but not at a D/P ratio of 0.1), prevents distamycin from getting its specific binding sites on DNA. At 320 nm, the CD amplitude associated with addition of distamycin should increase if the contributions of the two drugs were additive. Actually, the

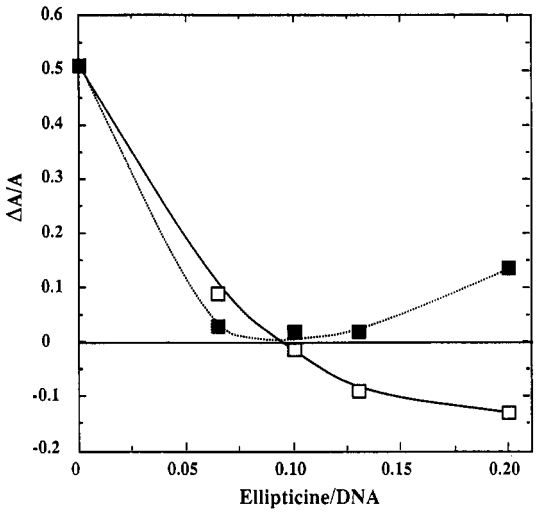

FIGURE 5: Dependence of reduced electric linear dichroism ($\Delta A/A$) on addition of the ellipticine derivative at a constant distamycin/DNA ratio of 0.1 (λ = 320 nm; E = 12.5 kV/cm) (open symbols). The dashed curve (filled symbols) corresponds to the calculated sum of the reduced dichroism measured separately for a distamycin–DNA complex (at D/P = 0.1) and for an ellipticine derivative–DNA complex at increasing D/P ratios.

CD signal at 320 nm decreases, showing that distamycin disturbs the intercalation of the ellipticine chromophore.

Variations in the CD amplitudes are much more pronounced in the reverse situation; when the ellipticine derivative is added to the distamycin–DNA complex (Figure 4b), a parallel decrease of the CD signal at 320 and 330 nm is observed until the ellipticine derivative/DNA ratio reaches 0.2. Therefore, when the ellipticine derivative is added to the solution, distamycin is partially displaced from its binding sites. The 320-nm CD signal remains constant at ellipticine derivative/DNA ratios above 0.13, while the 330-nm CD signal, mainly representative of distamycin binding, continues to decrease. To sum up, the competition experiments performed using either distamycin or the ellipticine derivative as competitor concur in demonstrating that the intercalating drug largely dominates over the minor-groove-binding drug in the binding reaction with DNA. However, it is also obvious that some simultaneous binding of the two drugs can effectively take place in spite of their differences in chemical structure, mode of binding (with consequent changes in DNA structure), and sequence selectivity.

(*B*) *Electric Linear Dichroism.* Progressive addition of the ellipticine derivative to a distamycin/DNA complex at a fixed D/P ratio of 0.1 causes the sign of the ELD signal at 320 nm to reverse (Figure 5). With equimolar concentrations of distamycin and the ellipticine derivative, i.e., at ellipticine derivative/DNA and distamycin/DNA ratios of 0.1, the ELD value is near zero, as expected from the algebraic sum of the dichroism amplitudes at 320 nm (see dashed curves in Figures 3 and 5) measured for individual ellipticine derivative–DNA and distamycin–DNA complexes. By contrast, at the same D/P ratio of 0.1, the Distel–DNA complex shows a dichroism value of –0.2. This suggests that when distamycin and ellipticine entities are integrated in the same hybrid structure, the ellipticine moiety dominates so as to fix the electric dichroism amplitude and consequently to set up the binding mode of the hybrid to DNA. When the ellipticine derivative/DNA ratio is increased to 0.2, the reduced dichroism falls to –0.17 while a dichroism value equal to +0.135 is calculated from the additive reduced dichroism values of the two individual drug–DNA complexes measured for the same D/P

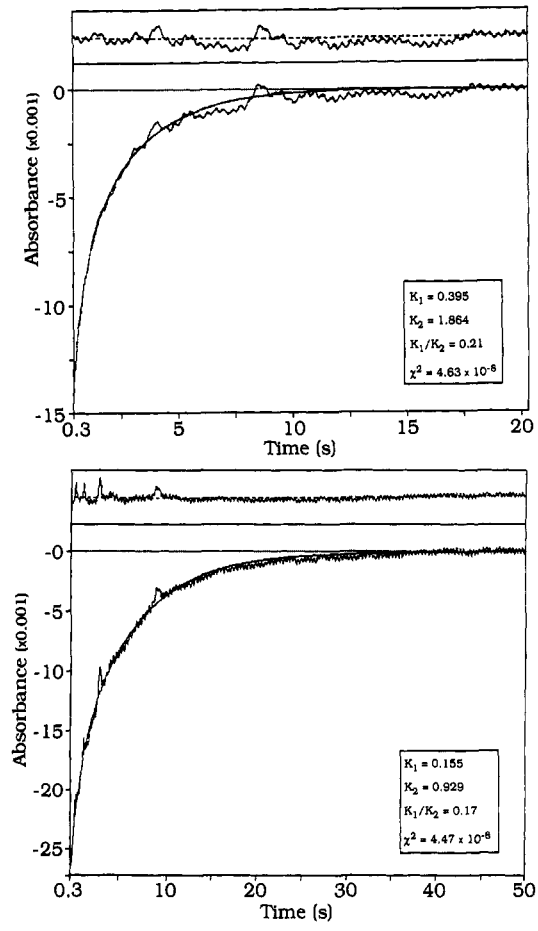

FIGURE 6: Representative stopped-flow kinetic traces of the absorbance change vs. time for the SDS-driven dissociation of Distel–DNA (top) and ellipticine–DNA (bottom) complexes at a D/P ratio of 0.1. Results are fitted to a two-exponential curve and plots of the residuals are shown. The fitted parameters are boxed.

ratios. These results suggest that the ellipticine chromophore, which must be partially externally bound to DNA at an ellipticine derivative/DNA ratio of 0.2 (Table I), hinders the location of distamycin in the DNA minor groove. Therefore, if the ellipticine does effectively disturb distamycin binding, it is not surprising to measure a similar negative dichroism amplitude ($\Delta A/A$ = –0.2 at 320 nm, Figure 3a) with the hybrid, i.e., when the two entities are directly tethered by a short aliphatic linker.

Stopped-Flow Kinetics. For all three compounds the drug–DNA association reaction is too rapid to be followed by stopped-flow techniques, but the SDS-driven dissociation kinetics can be measured under reasonable conditions except for distamycin, which dissociates from DNA very rapidly (total dissociation occurs in less than 3 ms). Stopped-flow traces for SDS-driven dissociation of the ellipticine derivative–DNA and Distel–DNA complexes are presented in Figure 6. The curves and residuals are given for dual-exponential fitting to the experimental data. Fitting with two exponentials gave a significant improvement compared to fits obtained with a single exponential. There was no significant change on going to a three-exponential fit. Similar biphasic curves have been reported for the dissociation kinetics of several anthracycline–DNA and anthraquinone–DNA complexes (Fox et al., 1985; Chaires et al., 1985; Gandecha et al., 1985; Krishnamoorthy et al., 1986), while the dissociation kinetics of simpler intercalating agents can often be fitted with a monoexponential curve [e.g., ethidium bromide (Wilson et al., 1985)].

We expected that significant kinetic stability would be imparted by the presence of a bulky DNA-binding substituent on the ellipticine ring. This prediction does not turn out to be verified experimentally since both rate constants are higher by a factor of 2 for Distel–DNA dissociation than for ellipticine derivative–DNA dissociation (i.e., dissociation of the hybrid–DNA complex occurs twice as fast as that of the ellipticine derivative–DNA complex). Evidently dissociation of the distamycin moiety does not constitute a rate-limiting step for release of the hybrid. This is another argument in favor of a slightly disturbed intercalation of the ellipticine part. On the other hand, the K_1/K_2 ratios for Distel and the ellipticine derivative are similar, suggesting that the dissociation mechanism may be much the same for both drugs. This situation is reminiscent of a study showing that variation in the structure of the side chain of the intercalating drug ametantrone had little effect on the kinetic stability of the complex (Denny & Wakelin, 1990).

Purines Hyperreactive to DEPC in the Presence of Distel. Diethyl pyrocarbonate (DEPC) forms a carbethoxylation adduct at the N7 position of purines so that subsequent treatment with hot piperidine leads to DNA strand cleavage (Nielsen, 1990). Adenosines, which are more reactive than guanosines, can be modified at the exocyclic N6 amino group as well (Johnston & Rich, 1985). The reactivity of purines is generally weak when DNA is in the B-conformation but becomes considerably enhanced when DNA adopts an altered conformation and in particular when the double helix is unwound by drugs (Portugal et al., 1988; McLean & Waring, 1988; Jeppesen & Nielsen, 1988). Thus, DEPC represents a very useful tool for probing variations in DNA structure and has been successfully applied to detect cruciform, B–Z junction, and numerous other variant conformations (Palecek, 1991).

The 253 base pair *Ava*I–*Pvu*II restriction fragment of the plasmid pBS has been subjected to DEPC treatment followed by piperidine workup, in the absence and presence of the hybrid Distel. As shown in Figure 7, the reactivity of purine residues is indeed enhanced in the presence of Distel. The reactivity of all purines along the DNA sequence is enhanced by the hybrid, but guanine residues are often much less strongly modified than adenines. The pattern of DEPC-enhanced sites found with Distel is very similar to that previously reported with the ellipticine derivative (Bailly et al., 1990a). The simplest explanation for the DEPC hypersensitivites sites is that binding of Distel alters the DNA structure in much the same fashion as the ellipticine derivative alone. Moreover, the extent of purine hypersensitivity is similar for the two ellipticine-containing drugs, again suggesting that they affect the conformation of DNA similarly, although their propensity to unwind the helix differs. Unwinding angles of 11° and 19° have been determined by topoisomerization assay for Distel and the ellipticine derivative, respectively (Bailly et al., 1992b). Distamycin, which does not unwind DNA upon binding, does not render DNA more susceptible to attack by DEPC.

However, it is now becoming clear that drug-induced hypersensitivity toward DEPC cannot be directly related to the unwinding effect of the ligand. This is borne out by the observation that the antibiotic actinomycin, which causes substantial unwinding of DNA (Waring, 1970), does not affect the DEPC-mediated cleavage pattern (Fox & Waring, 1984). What then, is the peculiar effect on DNA structure which is probed here by DEPC? These experiments cannot in themselves answer this question, but in conjunction with molecular modeling analysis we infer that enhanced DEPC-

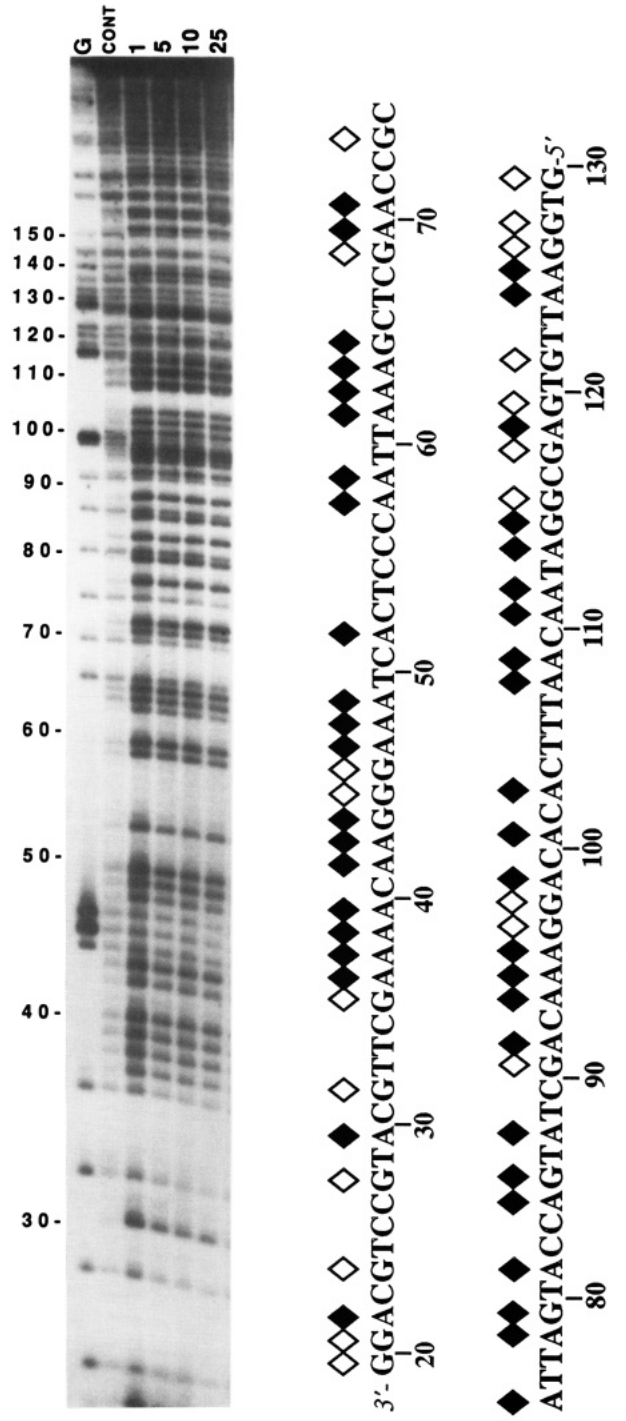

FIGURE 7: Diethyl pyrocarbonate reaction with the 253 base pair *Aval*–*Pvu*II restriction fragment of the plasmid pBS in the presence of different concentrations of Distel (1–25 μM). The tracts labeled CONT contained no drug. The track labeled G represents a dimethylsulfate–piperidine marker specific for guanine. The sites of hyperreactivity toward DEPC on the DNA fragment in the presence of 10 μM Distel are indicated on the sequence. Filled and open diamonds denote strong and weak sites of reactivity toward DEPC, respectively.

reactive sites occur, at least in part, as a result of ellipticine-induced DNA bending (vide infra).

Molecular Modeling by Energy Minimization. The molecular modeling study of the complex between the hybrid Distel and DNA was carried out with a DNA fragment eight base pairs long in which a central tract of four altering A·T base pairs is flanked by two alternating C·G base pairs on each side. This DNA fragment contains an AT-rich region which is known to provide a strong binding site for distamycin (Portugal & Waring, 1987), together with GC steps which provide strong binding sites for the ellipticine derivative (Bailly et al., 1990a). The conformational energy of energy-minimized ligand–DNA complexes can be decomposed into the following terms: (1) ΔE_{DNA} and ΔE_{LIG}, the deformation energy of DNA and ligand molecule, respectively, upon complex formation; (2) $E_{LIG-DNA}$, the ligand–DNA interaction energy, which is further split into Lennard–Jones (LJ) and electrostatic (Elec) components. E_{tot} is the sum of Lennard–Jones and electrostatic interactions. E_C is the energy of complex formation represented by the sum of ΔE_{DNA}, ΔE_{LIG}, and $E_{LIG-DNA}$.

Table II summarizes the characteristics of energy-minimized ligand–DNA complexes. In the best energy-minimized Distel–DNA complex, the distamycin moiety lies in the minor groove of the alternating A·T region with the ellipticine ring intercalated between the last A·T base pair and the next C·G base pair (Figures 8 and 9). The energy of the corresponding distamycin–DNA complex has been evaluated as well as that of two different complexes of DNA with the ellipticine derivative intercalated at the same site, i.e., at the 5′-TpG step, but with the side chain located in the minor groove or the major groove. The ellipticine derivative–DNA complex in which the attached aminopropyl chain is located in the minor groove is clearly favored. The driving force for this preference is the electrostatic interaction, which is stronger in the minor groove than in the major groove of double-stranded DNA. It is worth noting that binding of the ellipticine derivative side chain and Distel via minor-groove contacts is in agreement with other chemical studies which reveal that the reactivity of DNA toward dimethylsulfate and potassium tetrachloropalladinate is not affected by either ligand (not shown). These two chemical probes react with DNA via the major groove (Nielsen, 1990) and their access to DNA is apparently not hindered by any of the ligands tested here.

Therefore, it turns out that both distamycin and the aminopropyl side chain of the ellipticine derivative prefer to locate in the minor groove, so the conjugation of these two compounds might be expected to manifest some degree of synergy in their binding to DNA. Our preliminary modeling study suggested that the propyl linker should be flexible enough to permit simultaneous binding of both compounds. In this event, all four amino groups of the distamycin peptide bonds would form hydrogen bonds with the N3 atom of adenine or the O2 atom of thymine. The detailed analysis shows that the energy change associated with Distel–DNA interaction is increased by 28 kcal/mol (about 20%) compared to that of distamycin–DNA complexation (Table II). This increase is totally due to the Lennard–Jones component resulting from simultaneous intercalation of the ellipticine ring and groove binding of distamycin. However, the intercalation of ellipticine derivative demands a relatively high cost in terms of DNA deformation energy due to the unstacking of two consecutive base pairs at the intercalation site. As a result, the Distel–DNA complexation energy is very little different from that of the distamycin–DNA complex. This can be explained by the loss of two positive charges when distamycin and the ellipticine derivative are linked together. Thus the electrostatic contribution should be taken into account in future efforts to design conjugate molecules having high binding affinity for double-stranded DNA.

Figure 8 shows a structure of the best energy-minimized Distel–DNA complex. It can be seen that the double-stranded DNA fragment is bent toward the minor groove upon binding of the Distel conjugate. This structural change reflects the

Table II: Conformational Energy Decomposition of the Best Energy-Minimized Ligand–DNA Complexes

drug–DNA complexes	charges on ligand	ΔE_{DNA}	ΔE_{LIG}[b]	$E_{LIG-DNA}$[c]			E_C[d]
				LJ	elec	E_{tot}	
ellipticine derivative[e]	+2	+34.6	+2.3	−36.0	−53.8	−89.8	−52.9
ellipticine derivative[f]	+2	+29.4	+4.8	−42.8	−86.1	−128.9	−94.7
distamycin[g]	+1	+9.6	+10.8	−59.8	−68.8	−128.6	−108.2
Distel	+1	+34.2	+11.0	−88.3	−68.4	−156.7	−111.5
Distellip[h]	+2	+33.9	+15.7	−93.6	−99.9	−193.5	−143.9

[a] ΔE_{DNA} = deformation energy upon complexation of DNA. [b] ΔE_{LIG} = deformation energy upon complexation of the ligand. [c] $E_{LIG-DNA}$ = ligand–DNA interaction energy: LJ = Lennard-Jones component, elec = electrostatic component, and E_{tot} = LJ + elec. [d] $E_C = \Delta E_{DNA} + \Delta E_{LIG} + E_{LIG-DNA}$. [e,f] Two modes of orientation of the aminopropyl side chain of the ellipticine derivative, located in the major or minor groove of DNA, respectively. [g] The distamycin moiety is located in the minor groove at the central region of alternating A·T base pairs. [h] The computer-designed conjugate called Distellip is made by substituting the *N*-formyl group of Distel by a guanidinoacetyl group.

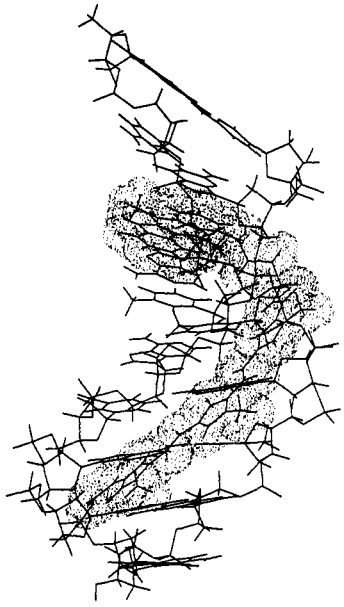

FIGURE 8: Structure from the minor groove of the best energy-minimized Distel–d(GCATATGC)$_2$ complex. Complex formation induces a pronounced DNA bending toward the minor groove in the vicinity of the ellipticine binding site.

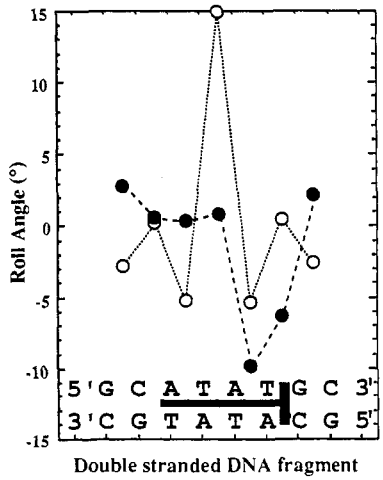

FIGURE 9: Variation of roll angles along the global helical axis of the uncomplexed (○) or Distel-complexed (●) double-stranded DNA fragment. The distamycin moiety is located in the minor groove associated with four alternating A·T base pairs, and the ellipticine ring is intercalated between the last A·T base pair and the next C·G base pair (schematized by a horizontal line and a thick vertical bar for distamycin and ellipticine moieties, respectively).

influence of the intercalated ellipticine ring since a similar bending of the double helix is produced by the ellipticine derivative alone. Distamycin does not show any such effect. On the contrary, distamycin strongly diminishes the bending of kinetoplast DNA (Wu & Crothers, 1984) and was found to decrease the bending of the sequence d(CGCAAATTTGCG) in the crystal structure of its distamycin complex by 4° (Coll et al., 1987). Figure 9 shows the variation of roll angles at each dinucleotide step of the uncomplexed and complexed DNA fragment. For the ligand-free octanucleotide, there is a large postive roll angle at the central 5′-TpA step corresponding to a local bending toward the major groove. But this bending is roughly compensated by the negative roll angles on both sides leading to an apparently straight DNA fragment. Upon Distel–DNA complex formation, two consecutive negative roll angles occur on the 5′ side of the TpG intercalation site of the ellipticine ring whereas the roll angle values of other base pairs remain near zero. This results in a pronounced drug-induced bending deformation of the DNA fragment.

An interesting link can be established between the molecular modeling analysis and the chemical reactivity–cleavage experiments. Indeed, we may logically argue that hyperreactivity of DNA toward DEPC attack observed in the presence of the ellipticine derivative and Distel (but not with distamycin) is accounted for by drug-induced bending of DNA revealed by the computer analysis. Hypersensitivity of DNA toward DEPC is a typical effect observed with a variety of mono- and bisintercalating drugs (Portugal et al., 1988; Fox & Grigg, 1988; McLean & Waring, 1988; Jeppesen & Nielsen, 1988). Most of the time, purine bases hyperreactive to DEPC are found all along the DNA fragment more or less independently of the location of the drug-binding sites. Thus DEPC reactivity experiments reveal that the conformation of DNA has changed upon drug binding, but it is generally not possible to determine the exact nature of the structural changes imposed by the drug. The multidisciplinary approach adopted here suggests that DEPC might be used as a tool for DNA bending investigation just as it is already used to detect other variant DNA conformations (Palecek, 1991).

Computer Design of a Distamycin–Ellipticine Conjugate. By comparing the energy of the different ligand–DNA complexes presented in Table II, it is clear that the stability of the distamycin–DNA complex is only marginally improved when the drug is linked to the intercalating chromophore. The energy of complex formation, E_C, is very similar for distamycin–DNA and Distel–DNA complexes. These computer-drawn findings are in agreement with the spectroscopic data reported in Table I, which show that the affinity of the hybrid for DNA is not superior to that of its parent compounds. The magnitude of the positive charge on the ligand seems to be critical for conferring high affinity for DNA.

To verify this hypothesis, molecular modeling analyses of a new distamycin–ellipticine hybrid molecule were undertaken. A guanidine group was introduced on the distamycin moiety

of Distel by replacing its *N*-formyl group with a guanidinoacetyl side chain, i.e., the cationic side chain of netropsin. Thus, this new conjugate called Distellip bears two positive charges instead of one as in the case of Distel. The additional positive charge of this hybrid should have a significant effect on the stability of the ligand–DNA complex. Indeed, the energy of complexation of Distellip–DNA is greatly improved with respect to that of the parent molecule Distel (Table II). The enhanced energy of the complex can be attributed directly to the increased electrostatic contribution. Such a biscationic distamycin–ellipticine hybrid, presently being synthesized, should be endowed with much higher affinity for DNA.

CONCLUSION

Absorption, circular and electric linear dichroism, stopped-flow kinetic measurements, chemical reactivity–cleavage experiments, and molecular modeling provide varied and complementary information about the mode of binding of the distamycin–ellipticine hybrid ligand to DNA. The combined approach has clearly shown that the ellipticine moiety of the conjugate dominates the DNA-binding reaction. Yet, from the spectroscopic results it is evident that the ellipticine–DNA and Distel–DNA intercalation complexes are slightly different. We suggest that when distamycin is linked to the intercalating ring, the overlap between the ellipticine chromophore and the DNA base pairs is diminished. The pyridine part of the pyridocarbazole ring, attracted by the appended tris(pyrrole) system, might protrude slightly away from the helix, thus placing the cationic site of the chromophore in the minor groove. This model accounts satisfactorily for both the lower kinetic stability and the lower unwinding angle measured with the Distel–DNA complex as compared to the ellipticine derivative–DNA complex.

The relationship postulated between the DEPC reactivity experiments and the molecular modeling analysis is quite interesting and may have relevance for a better understanding of the effect of ligands on DNA conformation upon binding. These analyses show that DNA can tolerate a variety of constraints so as to adopt a varied conformation that deviates significantly from the canonical Watson–Crick B-form. The conformational deformability inherent in DNA is considerably exploited by the present hybrid ligand. In fact, all (or almost all) DNA-binding ligands induce, to a more or less pronounced degree, distinctive and localized sequence-dependent perturbations of base pairing and conformation which very likely play a key role in their biological functions (Neidle et al., 1987).

In chromatin, the presence of histones does not disturb the minor-groove binding of distamycin but partially alters the intercalation of ellipticine derivative alone or integrated in Distel, especially by reducing the number of high-affinity sites. We also evidence a preference for binding to linker DNA in the order ellipticine derivative > Distel > distamycin, illustrating again that the two constituents of the hybrid exhibit some mutual interference, even in their binding to chromatin.

In summary, the distamycin–ellipticine hybrid ligand Distel has retained most of the binding properties of the ellipticine moiety alone. The molecular combination of two entities with very different binding affinities for DNA leads to a hybrid molecule whose binding affinity for DNA is more or less similar to that of the entity presenting the highest affinity for DNA. Future design of hybrid ligands should consider use of a minor-groove binder able to bind to DNA as tightly as the intercalating chromophore (e.g., the use of a distamycin moiety bearing an additional positive charge). In these conditions, the binding constant may be multiplicative (i.e., the affinity constant of the hybrid for DNA may be equal to the product $K_{\text{intercalator}}K_{\text{minor-groove binder}}$). In the case of Distel, intercalation appears to be the crucial element. This situation differs markedly from that previously reported with a netropsin–acridine hybrid ligand, whose binding to DNA and chromatin appeared to be mostly influenced by its minor-groove-binding part (Bailly et al., 1989, 1990b, 1992a). Therefore, depending on the nature of the coupled drugs and of the DNA sequences, one or the other of the two binding modes can predominate. Just as there is considerable structural and functional diversity within natural DNA ligands, so there will be diversity among hybrids.

ACKNOWLEDGMENT

The authors are grateful to Denis Vandesande for his skillful assistance.

REFERENCES

Arnott, S., Chandrasekharan, R., Birdsall, D. L., Leslie, A. G. W., & Ratliff, R. L. (1980) *Nature 283*, 743–746.

Bailly, C., & Hénichart, J. P. (1991) *Bioconjugate Chem. 2*, 379–393.

Bailly, C., Pommery, N., Houssin, R., & Hénichart, J. P. (1989) *J. Pharm. Sci. 78*, 910–917.

Bailly, C., OhUigin, C., Rivalle, C., Bisagni, E., Hénichart, J. P., & Waring, M. J. (1990a) *Nucleic Acids Res. 15*, 491–507.

Bailly, C., Helbecque, N., Colson, P., Houssier, C., Rao, K. E., Shea, R. G. Lown, J. W., & Hénichart, J. P. (1990b) *J. Mol. Recognit. 3*, 26–35.

Bailly, C., Collyn-d'Hooghe, M., Lantoine, D., Fournier, C., Hecquet, B., Fosse, P., Saucier, J. M., Colson, P., Houssier, C., & Hénichart, J. P. (1992a) *Biochem. Pharmacol. 43*, 457–466.

Bailly, C., OhUigin, C., Houssin, R., Colson, P., Houssier, C., Rivalle, C., Bisagni, E., Hénichart, J. P., & Waring, M. J. (1992b) *Mol. Pharmacol. 41*, 845–855.

Bailly, C., Denny, W. A., Mellor, L. E., Wakelin, L. P. G., & Waring M. J. (1992c) *Biochemistry 31*, 3514–3524.

Chaires, J. B., Dattagupta, N., & Crothers, D. M. (1985) *Biochemistry 24*, 260–267.

Coll, M., Frederick, C. A. Wang, A. H.-J. & Rich, A. (1987) *Proc. Natl. Acad. Sci. U.S.A 84*, 8385–8389.

Denny, W. A., & Wakelin, L. P. G. (1990) *Anti-Cancer Drug Des. 5*, 189–200.

Ducrocq, C., Wendling, F., Tourbez-Perrin, M., Rivalle, C., Tambourin, P., Pochon,, F., & Bisagni, E. (1980) *J. Med. Chem. 23*, 1212–1216.

Fox, K. R., & Waring, M. J. (1984) *Nucleic Acids Res. 12*, 9271–9285.

Fox, K. R., & Grigg, G. W. (1988) *Nucleic Acids Res. 16*, 2063–2075.

Fox, K. R., Brassett, C., & Waring, M. J. (1985) *Biochim. Biophys. Acta 840*, 383–392.

Fredericq, E., & Houssier, C. (1972) *Biopolymers 11*, 2281–2308.

Fredericq, E., & Houssier, C. (1973) in *Electric dichroism and electric birefringence*, Clarendon Press, Oxford, England.

Gandecha, B. M., Brown, J. R., & Crampton, M. R. (1985) *Biochem. Pharmacol. 34*, 733–742.

Hagmar, P., Marquet, R., Colson, P., Kubista, M., Nielsen, P., Norden, B., & Houssier, C., (1989) *J. Biomol. Struct. Dyn. 7*, 19–33.

Hagmar, P., Pierrou, S., Nielsen, P. E., Nordén, B., & Kubista, M. (1992) *J. Biomol. Struct. Dyn. 9*, 667–679.

Hartwell, J., & Abbott, B. (1969) *Adv. Pharmacol. Chemother, 7*, 117–209.

Houssier, C. (1981) in *Molecular Electro-Optics* (Krause, S., Ed.) NATO ASI Series B, Vol. 64, pp 363–398, Plenum Publishing Corp., New York.
Houssier, C., Hardey, B., & Fredericq, E. (1974) *Biopolymers 13*, 1141–1160.
Jeppesen, C., & Nielsen, P. E. (1988) *FEBS Lett. 231*, 172–176.
Johnston, B. H., & Rich, A. (1985) *Cell 42*, 713–724.
Kohn, K. W., Waring, M. J., Glaubiger, D., & Friedman, C. A. (1975) *Cancer Res. 35*, 71–76.
Krishnamoorthy, C. R., Yen, S. F., Smith, J. C., Lown, J. W., & Wilson, W. D. (1986) *Biochemistry 25*, 5933–5940.
Kubista, M., Härd, T., Nielsen, P. E., & Nordén, B. (1985) *Biochemistry 24*, 6336–6342.
Larue, L., Quesne, M., & Paoletti, J. (1987) *Biochem. Pharmacol. 36*, 3563–3569.
Larue, L., Rivalle, C., Muzard, G., Paoletti, C., Bisagni, E., & Paoletti, J. (1988) *J. Med. Chem. 31*, 1951–1956.
Lavery, R. (1988) in *Structure and Expression, Volume 3: DNA Bending and Curvature.* (Olson, W. K., Sarma, M. H., Sarma, R. H., & Sundaralingam, M., Eds.) pp 191–211, Adenine Press, Guilderland, NY.
Lavery, R., & Sklenar, H. (1989) *J. Biomol. Struct. Dyn. 6*, 655–667.
Lavery, R., Zakrzewska, K., & Pullman, A. (1984) *J. Comput. Chem. 5*, 363–373.
Lavery, R., Sklenar, H., Zakrzewska, K., & Pullman, A. (1986) *J. Biomol. Struct. Dyn. 3*, 989–1014.
Leatherbarrow, R. J. (1990) *Trends Biochem. Sci. 15*, 455–458.
Le Doan, T., Perrouault, L., Asseline, U., Thuong, N. T., Rivalle, C., Bisagni, E., & Hélène, C. (1991) *Antisense Res. Dev. 1*, 43–54.
Le Pecq, J. B., Dat Xuong, N., Gosse, C., & Paoletti, C. (1974) *Proc. Natl. Acad. Sci. U.S.A. 71*, 5078–5082.
Luck, G., Zimmer, C., Reinert, K. E., & Arcamone, F. (1977) *Nucleic Acids Res. 4*, 2655–2670.
McGhee, J. D., & von Hippel, P. H. (1974) *J. Mol. Biol. 86*, 469–489.
McLean, M. J., & Waring, M. J. (1988) *J. Mol. Recognit. 1*, 138–151.
McMurray, C. T., & van Holde, K. E. (1986) *Proc. Natl. Acad. Sci. U.S.A. 83*, 8472–8476.
McMurray, C. T., & van Holde, K. E. (1991) *Biochemistry, 30*, 5631–5642.
Müller, W., & Crothers, D. M. (1968) *J. Mol. Biol. 35*, 251–290.
Neidle, S., Pearl, L. H., & Skelly, J. V. (1987) *Biochem. J. 243*, 1–13.
Nielsen, P. E. (1990) *J. Mol. Recognit. 3*, 1–25.
Palecek, E. (1991) *Crit. Rev. Biochem. Mol. Biol. 26*, 151–226.
Paoletti, C., Lesca, C., Cros, S., Malvy, C., & Auclair, C. (1979) *Biochem. Pharmacol. 28*, 345–350.
Perrouault, L., Asseline, U., Rivalle, C., Thuong, N. T., Bisagni, E., Giovannangeli, C., Le Doan, T., & Hélène, C. (1990) *Nature 344*, 358–360.
Portugal, J., & Waring, M. J. (1987) *Eur. J. Biochem. 167*, 281–289.
Portugal, J., Fox, K. R., McLean, M. J., Richenberg, J. L., & Waring, M. J. (1988) *Nucleic Acid Res. 16*, 3655–3670.
Schwaller, M. A., Aubard, J., Auclair, C., Paoletti, C., & Dodin, G. (1989) *Eur. J. Biochem. 181*, 129–134.
Smith, J. M., & Thomas, D. J. (1990) *Comput. Appl. Biosci. 6*, 93–99.
Waring, M. J. (1970) *J. Mol. Biol. 54*, 247–279.
Wilson, W. D., Krishnamoorthy, C. R., Wang, Y. H., & Smith, J. C. (1985) *Biopolymers 24*, 1941–1961.
Wu, H.-M & Crothers, D. M. (1984) *Nature 308*, 509–513.
Zimmer, C. (1975) *Prog. Nucleic Acids Res. Mol. Biol. 15*, 287–318.
Zimmer, C., & Wähnert, U. (1986) *Prog. Biophys. Mol. Biol. 47*, 31–112.
Zwelling, L. A., Michaels, S., Kerrigan, D., Pommier, Y., & Kohn, K. W. (1982) *Biochem. Pharmacol. 31*, 3261–3267.